# Thermal-radiation-induced nonequilibrium carriers in intrinsic graphene

P. N. Romanets, F. T. Vasko,* and M. V. Strikha
*Institute of Semiconductor Physics, NAS of Ukraine, Pr. Nauky 41, Kyiv, 03028, Ukraine*
(Received 22 August 2008; revised manuscript received 8 December 2008; published 14 January 2009)

We have examined an intrinsic graphene connected to the phonon thermostat at temperature $T$ under irradiation of thermal photons with temperature $T_r$, different from $T$. The distribution of nonequilibrium electron-hole pairs was obtained for the cases when the interparticle scattering is unessential and when the Coulomb scattering dominates. For the first case, the distribution function is determined by the interplay of intraband relaxation of energy due to acoustic phonons and interband radiative transitions caused by the thermal radiation. For the alter case, the quasiequilibrium distribution with effective temperature and nonequilibrium concentration, determined through balance equations, is realized. Due to the effect of thermal radiation with temperature $T_r \neq T$, concentration and conductivity of carriers in graphene are modified essentially. It is demonstrated that at $T_r > T$, the negative interband absorption caused by the inversion of carriers distribution can occur.

DOI: 10.1103/PhysRevB.79.033406 PACS number(s): 73.50.Fq, 73.63.−b, 81.05.Uw

Different kinetic phenomena caused by carriers localized near the band cross point of graphene, including dc (magneto)transport and optical properties, have been studied intensively within recent years (see reviews[1] and last references in Refs. 2 and 3). The main attention was paid to examination of linear response of the carriers in the phonon thermostat at temperature $T$. Because of the weak carrier interaction with acoustic phonons[4] different external factors can easily disturb the equilibrium of electron-hole system, and the linear-response behavior realization requires a strict control. In particular, when the sample is not isolated from external thermal radiation with temperature $T_r \neq T$, the carriers interaction with the additional thermostat of thermal photons is essential. This interaction can be effective enough because the interband transitions are determined by the matrix element with the velocity $v_W = 10^8$ cm/s characterizing the linear spectrum of carriers (the neutrinolike states near the band-crossing point are described by the Weyl-Wallace model[5]). Therefore, graphene is very sensitive to thermal irradiation: the concentration and conductivity of carriers can be modified essentially (particularly, the photoconductivity induced by thermal irradiation occurs, compare with,[6] where the case of the interband pumping was discussed).

In this Brief Report, the results for the distribution of nonequilibrium carriers in the intrinsic graphene, interacting with phonon and photon thermostats at different temperatures, are presented. This distribution is obtained from the kinetic equation, taking into consideration the quasielastic energy relaxation due to acoustic phonons, generation-recombination processes due to interband transitions, caused by thermal irradiation (the corresponding collision integrals were obtained in Ref. 6) and the carrier-carrier scattering, which does not cause the interband transitions, see Ref. 7. Moreover, the scattering by static disorder should be taken into account as the main mechanism of momentum relaxation.[8] If the Coulomb scattering is unessential, the distribution function differs essentially from equilibrium one due to interplay between acoustic scattering and radiative transitions. When the Coulomb scattering dominates, the quasiequilibrium distribution of carriers with effective temperature and nonequilibrium concentration is imposed. We also calculate the dependences of concentration and conductivity on $T$ and $T_r$ under the scattering by the finite-range static disorder.

In the intrinsic graphene with the symmetrical $c$ and $v$ bands, and with similar scattering in these bands, the distributions of electrons and holes are identical; they are described by distribution function $f_p$. This function is governed by the quasiclassical kinetic equation,[6,9]

$$J_{LA}(f|p) + J_R(f|p) + J_C(f|p) = 0. \tag{1}$$

Here the collision integrals $J_{LA}$, $J_R$, and $J_C$ describe the relaxation of carriers caused by the phonon ($LA$) and photon ($R$) thermostats and the carrier-carrier scattering ($C$), respectively. The solutions of Eq. (1) have been obtained below for the two cases: (a) when the intercarrier scattering $J_C$ can be neglected, and (b) when $J_C$ imposes the quasiequilibrium distribution with parameters determined from the equations of the balance of concentration and energy. The concentration and energy density, $n$ and $E$, are determined by standard relations,

$$\begin{vmatrix} n \\ E \end{vmatrix} = \frac{2}{\pi\hbar^2}\int_0^\infty dpp \begin{vmatrix} 1 \\ v_W p \end{vmatrix} f_p. \tag{2}$$

After summation of Eq. (1) over $\mathbf{p}$ plane with the weights 1 and $v_W p$ we get these balance equations in the form,[6,9]

$$\frac{4}{L^2}\sum_{\mathbf{p}} J_R(f|p) = 0, \tag{3}$$

$$\frac{4}{L^2}\sum_{\mathbf{p}} v_W p[J_{LA}(f|p) + J_R(f|p)] = 0, \tag{4}$$

where $L$ is normalizing length and the contribution of acoustic scattering is omitted in the equation of the concentration balance because the interband transitions are forbidden due to the inequality $s \ll v_W$, where $s$ is the sound velocity. Note that the intercarrier scattering does not change the concentration and energy.[7,9]

We start with the examination of the case, when the intercarrier collision integral $J_C$ in Eq. (1) can be neglected. With the use of collision integrals $J_{LA}$ and $J_R$, presented in Ref. 6,

 

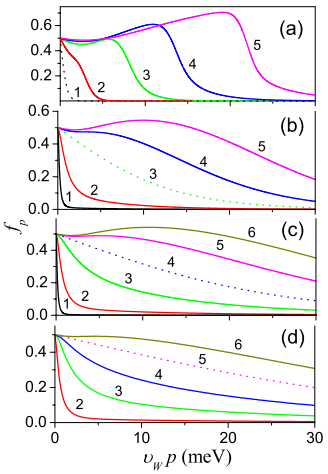


FIG. 1. (Color online) Distribution functions governed by Eq. (5) for the cases: (a) $T=4.2$ K, (b) $T=77$ K, (c) $T=150$ K, and (d) $T=250$ K at (1) $T_r=4.2$ K, (2) 20 K, (3) 77 K, (4) 150 K, (5) 250 K, and (6) 350 K. Dotted curves are the equilibrium thermal distributions at $T=T_r$.

with temperatures $T$ and $T_r$ correspondingly, we get the nonlinear equation of the second order for the distribution function $f_p$:

$$\frac{\nu_p^{(\mathrm{qe})}}{p^2}\frac{d}{dp}\left\{p^4\left[\frac{df_p}{dp}+\frac{f_p(1-f_p)}{p_T}\right]\right\} + \nu_p^{(r)}[N_{2p/p_r}(1-2f_p)-f_p^2]=0. \quad (5)$$

Here we introduce the characteristic momenta $p_T=T/v_W$ and $p_r=T_r/v_W$; $N_{2p/p_r}=[\exp(2p/p_r)-1]^{-1}$ is the Planck function. The rates of quasielastic relaxation at acoustic phonons, $\nu_p^{(\mathrm{qe})}=(s/v_W)^2 v_{\mathrm{ac}} p/\hbar$, and radiative transitions, $\nu_p^{(r)}=v_r p/\hbar$, have been expressed through the characteristic velocities, $v_{\mathrm{ac}}$ and $v_r$. They separate the momentum dependence of the relaxation rates, which is proportional to the density of states. According to Vasko and Ryzhii,[8] where the temperature dependence of mobility have been examined, $v_{\mathrm{ac}}\simeq 1.35\times 10^4$ cm/s for the helium temperature (moreover $v_{\mathrm{ac}}\propto T$), and the quasielastic character of scattering is determined by the small parameter $s/v_W$. For graphene placed between the $SiO_2$ substrate and cover layer, we get $v_r\simeq 41.6$ cm/s, see Ref. 6.

The boundary conditions for Eq. (5) are imposed both by the concentration balance Eq. (3) and by the requirement $f_{p\to\infty}=0$, which is transformed into $p^4(df_p/dp+f_p)_{p\to\infty}<\mathrm{const}$. Because the acoustic and radiative contributions become zero under the equilibrium contributions with temperatures $T$ and $T_r$ correspondingly, and these two contributions trend to 1/2 at small $p$, we get $f_{p\to 0}=1/2$.[10] This demand can be used as the boundary condition for the numerical solution of Eq. (5). Note, that the validity of Eq. (3) for the obtained distribution should be examined. This solution was obtained below with the use of the finite difference method and the iterations over nonlinear contributions in Eq. (5), see Ref. 11.

In Figs. 1(a)–1(d) the obtained distribution functions versus energy $v_W p$ for different $T$ and $T_r$ are presented. Due to the smallness of acoustic contribution at $p\to 0$ (see above), $f_p$ is close to equilibrium distribution with the temperature $T_r$. If $T_r>T$ the distribution increases at high energies up to the range, where $J_{LA}$ is dominant. With the further increase in $v_W p$ the distribution decreases rapidly on the scale of energies $T$ so that the peak of distribution is formed at the energies $\sim T_r$; this peak causes the carriers concentration of the order of equilibrium value at the temperature $T_r$. In this case the condition $f_{\max}>1/2$ is realized, i.e., the inverse distribution of the carriers occupation takes place for the energies close to the maximum of distribution (see below). On the contrary, if $T_r<T$, the equilibrium contribution of the slow carriers is replaced by the rapidly decreasing part in the range of $v_W p<T$. This distribution determines the small concentration of carriers in comparison with the equilibrium value at the temperature $T$.

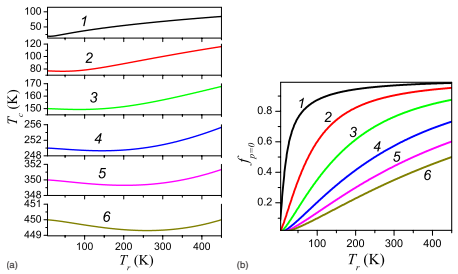


FIG. 2. (Color online) (a) Effective temperature $T_c$ and (b) maximal distribution $\tilde{f}_{p=0}$ versus $T_r$ for different temperatures (1) $T=20$ K, (2) 77 K, (3) 150 K, (4) 250 K, (5) 350 K, and (6) 450 K.

Later we shall examine the case, when the Coulomb scattering dominates, imposing the quasiequilibrium distribution,

$$\tilde{f}_p=\{\exp[(v_W p-\mu)/T_c]+1\}^{-1}. \quad (6)$$

The effective temperature of carriers $T_c$ and the chemical potential $\mu$ in this distribution are obtained from the balance Eqs. (3) and (4). After introducing the dimensionless momentum $x=v_W p/T_c$, we get the concentration balance equation,

$$\int_0^\infty dx x^2\left(\frac{1-2\tilde{f}_x}{e^{2xT_c/T_r}-1}-\tilde{f}_x^2\right)=0, \quad (7)$$

which imposes the relation between $\mu$ and $T_c/T_r$, while the phonon temperature is omitted in this equation. In these variables the energy balance equation can be presented as

$$\int_0^\infty dx x^3\left(\frac{1-2\tilde{f}_x}{e^{2xT_c/T_r}-1}-\tilde{f}_x^2\right)-\gamma\frac{T_c-T}{T}\int_0^\infty dx x^4 e^{x-\mu/T_c}\tilde{f}_x^2=0, \quad (8)$$

where $\gamma=(s/v_W)^2 v_{ac}/v_r\propto T$ determines the relative contribution of the phonon and photon thermostats.

The solution of the transcendental Eqs. (7) and (8) gives the distribution [Eq. (6)], dependent on $T$ and $T_r$, which can be characterized by the effective temperature $T_c$, and the maximum value of the function $\tilde{f}_{p=0}=[\exp(-\mu/T_c)+1]^{-1}$. These values are presented in Fig. 2. If $T>150$ K, one can see that the temperature $T_c$ differs from $T$ unessentially under

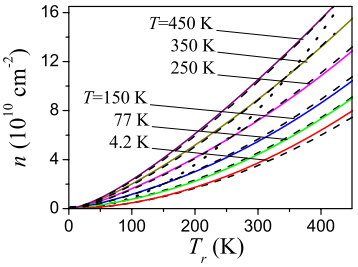


FIG. 3. (Color online) Carrier concentrations given by Eq. (10) versus temperature $T_r$ for different $T$. Solutions of Eq. (5) and of the balance Eqs. (7) and (8) are plotted by dashed and solid curves. The equilibrium concentration (if $T=T_r$) is shown as dotted curve.

the great change of $T_r$, meanwhile $\mu$ and $\tilde{f}_p$ modify essentially for the temperature range up to 450 K (the high-temperature measurements of graphene were carried out recently[12]). The essential difference between the case under examination and the low-temperature solution case, presented in Fig. 1, is that the value $f_{p=0}$ is being fixed (and equal to 1/2), while the value $\tilde{f}_{p=0}$ decreases with the increase of $T$, and increases with the increase of $T_r$; note that $\tilde{f}_{p=0}=1/2$ when $T=T_r$.

As one can see from Figs. 1 and 2(b), distribution $f_p$ or $\tilde{f}_p$ can be greater than 1/2 in a certain energy range or at low energies. Since the inversion of electron-hole pairs occupation, the regime of the negative interband absorption can occur because the real part of dynamic conductivity is given by the expression,[3]

$$\mathrm{Re}\ \sigma_\omega = (e^2/4\hbar)(1-2f_{p_\omega}), \tag{9}$$

where $p_\omega=\hbar\omega/v_W$. In the range of parameters, when $f_p$ or $\tilde{f}_p>1/2$, the intrinsic graphene tends to be unstable if an additional adsorption is weak enough.

The distributions presented in Figs. 1 and 2 are used below for describing the nonequilibrium response (concentration, energy density, and conductivity). The nonequilibrium concentration $n$, which is dependent on $T$ and $T_r$, is given by the standard expression

$$n=(2/\pi\hbar^2)\int_0^\infty dppf_p=(2/\pi)(T_c/\hbar v_W)^2\int_0^\infty dxx\tilde{f}_x, \tag{10}$$

where the right equality was written under the substitution of Eq. (6) into the general formula. In Fig. 3 we plot $n$ versus $T$ and $T_r$ for the two cases, when the Coulomb scattering can either be neglected, or it dominates. At $T=T_r$ these curves intersect with equilibrium concentration $\propto T^2$ because the concentration is controlled by thermal irradiation, $n$ is smaller (or greater) than the equilibrium concentration at $T<T_r$ (or $T>T_r$). Note that the dependences obtained from Eq. (5) and from the equations of balance [Eqs. (7) and (8)] correspond well for all concentrations because the intercarrier scattering does not change concentration.

The energy density, $E$, is determined from Eq. (2) as follows,

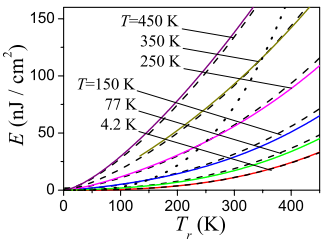


FIG. 4. (Color online) Energy density given by Eq. (11) versus temperature $T_r$ for different $T$. Solutions of Eq. (5) and of the balance Eqs. (7) and (8) are plotted by dashed and solid curves. The equilibrium concentration (if $T=T_r$) is shown as dotted curves.

$$E=(2v_W/\pi\hbar^2)\int_0^\infty dpp^2f_p=(2T_c/\pi)(T_c/\hbar v_W)^2\int_0^\infty dxx^2\tilde{f}_x, \tag{11}$$

where the quasiequilibrium distribution [Eq. (6)] used in the right equality. In Fig. 4 we plot $E$ versus $T$ and $T_r$ using the solution obtained from Eq. (5) and the quasiequilibrium distribution [Eq. (6)] with parameters obtained from Eqs. (7) and (8). We also plot the equilibrium energy density obtained under the condition $T=T_r$, which is proportional to $T^3$. Once again, $E$ is smaller (or greater) than the equilibrium energy density at $T<T_r$ (or $T>T_r$). Similar to Fig. 3, the dependencies obtained for the both cases under consideration are in good agreement because the Coulomb scattering does not change energy of carriers.

The modifications of the distribution of nonequilibrium carriers in the intrinsic graphene, described above, lead to modification of conductivity, $\sigma$. For the scattering of momenta due to static disorder with correlation length $l_c$, we calculate the conductivity using the expression,[9]

$$\sigma=\sigma_0\left[2f_{p=0}-\frac{l_c}{\hbar}\int_0^\infty dpf_p\frac{\Psi'(pl_c/\hbar)}{\Psi(pl_c/\hbar)^2}\right], \tag{12}$$

where $\Psi(z)=\exp(-z^2)I_1(z^2)/z^2$ is written through the first-order Bessel function of the imagined argument, $I_1(z)$, and $\sigma_0$ is the conductivity in the case of short-range disorder scattering, when $l_c=0$. For the case of short-range scattering, $\bar{p}l_c/\hbar\ll 1$ ($\bar{p}$ is the characteristic momentum of nonequilibrium carriers) the conductivity can be expressed through low-temperature distribution: $\sigma\simeq 2\sigma_0 f_{p=0}$. Therefore the conductivity obtained for the cases ($a$) and ($b$) differ essentially for the the low-temperature range; in the case without intercarrier scattering, when $f_{p\to 0}=1/2$, the conductivity depends weakly on $T$ and $T_r$, but under Coulomb control, when $f_{p\to 0}=0$, the conductivity is vanished. In the intermediate range of temperatures (and concentrations) the results correspond well for the both cases [see Figs. 5(a) and 5(b)]. In the range of high temperatures the difference between the results arise again because the distribution becomes zero at high energies under Coulomb control. In Fig. 5(b) we present the dependence $\sigma/\sigma_0$ versus $T$ for different $T_r$. This dependence demonstrates the correlation of the results in the intermediate range. In this case, when the intercarrier scattering is dominant, $\sigma$ is less sensitive to the scattering suppress due to the

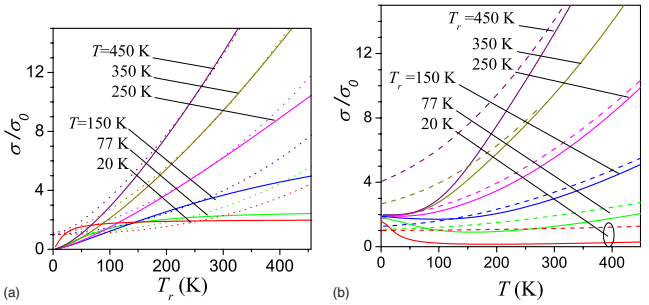


FIG. 5. (Color online) (a) Normalized conductivity, $\sigma/\sigma_o$, at $l_c=20$ nm versus radiation temperature $T_r$ for different $T$. (b) The same versus phonon temperature $T$ for different $T_r$.

finiteness of $l_c$ (see Figs. 5 and 6). The temperature dependences of conductivity depend essentially on the correlation length as well. With the increase in $l_c$ the second term in Eq. (12) becomes essential and the thermal dependences $\sigma/\sigma_o$ become much stronger; see Fig. 6.

Next, we discuss the assumptions used. The main restriction is that instead of a complete solution of Eq. (1) we examine the two limit cases either of no intercarrier collisions or of their domination only. The strict solution of the problem should be somewhere between the solutions obtained above, therefore the approach being used is effective when these solutions are close one to another. Moreover such characteristics as concentration and energy density are not sensitive to the nonequilibrium distribution peculiarities (see Figs. 3 and 4) because the Coulomb scattering does not change the concentration of carriers and their energy. The situation for conductivity is more complicated; despite the results correspond well in the wide intermediate range of temperatures, the approximations being used lead to different results in the low- and high-temperature ranges (see Figs. 5 and 6). The accurate analysis of these temperature ranges should take into account the strict consideration of intercarrier scattering. However, this is beyond of the scope of our Brief Report.

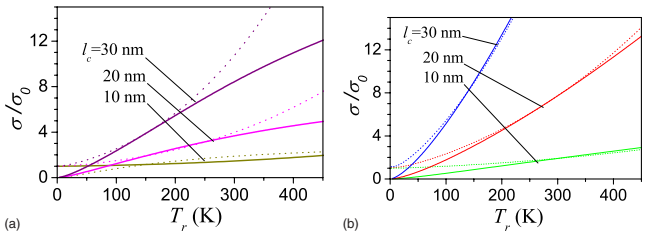


FIG. 6. (Color online) (a) Normalized conductivity, $\sigma/\sigma_o$, versus $T_r$ for $T=150$ K at different correlation lengths, $l_c$. (b) The same for $T=300$ K.

Other assumptions are rather standard for the calculations of the transport phenomena in graphene. We use linear approximation for carrier dispersion, and we consider electrons and holes spectra, as well as their scattering parameters, as symmetric ones. Under calculation of conductivity the phenomenological model of momentum relaxation, proposed in Ref. 9, was used; despite that, it corresponds well the experimental data,[1,12] and the microscopic mechanisms of scattering are still unclear.[13] The parameters, which determine the energy relaxation, correspond to these being discussed in Ref. 14, the radiative generation-recombination transitions only were taken into consideration. This mechanism is described on the basis of the well-known optical properties of graphene,[3,15] while the problem of the possible radiationless channels of interband transitions is still opened.

In closing, the consideration performed demonstrates the essential effect of thermal irradiation on the intrinsic graphene properties, therefore the transport measurements should be carried under the accurate control of the condition $T=T_r$, otherwise the carriers are nonequilibrium, and the results can depend on noncontrolled external conditions that determine $T$ and $T_r$. Within the study of the device applications we should also consider the possible difference between the temperature of phonons and the temperature of the external thermal radiation.

*ftvasko@yahoo.com

[1] A. H. Castro Neto *et al.*, arXiv:0709.1163, Rev. Mod. Phys. (to be published); A. K. Geim and A. H. MacDonald, Phys. Today **60**, 35 (2007).
[2] K. I. Bolotin *et al.*, Phys. Rev. Lett. **101**, 096802 (2008).
[3] R. R. Nair *et al.*, Science **320**, 1308 (2008); T. Stauber, N. M. R. Peres, and A. K. Geim, Phys. Rev. B **78**, 085432 (2008).
[4] The optic phonons are freezed out at $T \ll 0.2$ eV, therefore they are unessential even for the temperatures, higher than the room one.
[5] E. M. Lifshitz, L. P. Pitaevskii, and V. B. Berestetskii, *Quantum Electrodynamics* (Butterworth-Heinemann, Oxford, 1982); P. R. Wallace, Phys. Rev. **71**, 622 (1947).
[6] F. T. Vasko and V. Ryzhii, Phys. Rev. B **77**, 195433 (2008).
[7] L. Fritz *et al.*, Phys. Rev. B **78**, 085416 (2008); M. Muller *et al.*, *ibid.* **78**, 115406 (2008).
[8] F. T. Vasko and V. Ryzhii, Phys. Rev. B **76**, 233404 (2007).
[9] F. T. Vasko and O. E. Raichev, *Quantum Kinetic Theory and Applications* (Springer, NY, 2005).
[10] In order to check the condition $f_{p\to 0}=1/2$ we have examined the transient process of the formation of the steady-state distribution, described by the equation $\partial f_{pt}/\partial t = J_{LA}(f_t|p)+J_R(f_t|p)$ with the initial condition $t_{pt=0}=[\exp(p/p_T)+1]^{-1}$. The numerical computation of the Cauchy problem with the use of time iterations method gives the same steady-state distribution, as in Fig. 1.
[11] D. Potter, *Computational Physics* (J. Wiley, London, 1973).
[12] Q. Shao *et al.*, Appl. Phys. Lett. **92**, 202108 (2008).
[13] T. M. Mohiuddin *et al.*, arXiv:0809.1162; S. Adam *et al.*, arXiv:0811.0609.
[14] S. V. Morozov *et al.*, Phys. Rev. Lett. **100**, 016602 (2008); E. H. Hwang and S. Das Sarma, Phys. Rev. B **77**, 115449 (2008).
[15] L. A. Falkovsky, Phys. Usp. **51**, 887 2008.